Journal of Solid State Chemistry **163,** 202–209 (2002)
doi:10.1006/jssc.2001.9393, available online at http://www.idealibrary.com on IDEAL®

Reactions of Metal Salts and Alkali Metal Nitrates. Role of the Metal Precursors and Alkali Metal Ions in the Resulting Phase of Zirconia

Pedro Marote,* Bernard Durand,† and Jean-Pierre Deloume‡,[1]

*Laboratoire de Chimiométrie, ERT n° 11, UCB Lyon 1, France; †CIRIMAT-LCMIE, UMR n° 5085, UPS, 118 rte de Narbonne, F- 31062 Toulouse cedex, France; ‡LACE, UMR n° 5634, UCB Lyon 1, 43 Bd du 11 Novembre, F-69622 Villeurbanne cedex, France

Received May 16, 2001; in revised form August 28, 2001; accepted September 7, 2001

Zirconia powders are prepared by reaction of a zirconium precursor with an alkali metal nitrate. The major part of the reactions takes place before the melting points and then the reactions go slowly to completion at 450°C in the molten salts. The roles of the precursor and the alkali metal ion are discussed considering the reaction between two precursors, octahydrated zirconium oxychloride and zirconium tetrachloride, and two nitrates, $LiNO_3$ and $NaNO_3$, and some resulting physico-chemical differences. The obtained zirconia powders contain very small amounts of alkali metal ions which act as stabilizing agent. Their effect on the balance tetragonal–monoclinic ZrO_2 depends upon the homogeneity of their distribution which is related to their ability to diffuse inside the bulk of particles and their polarizing power when located mainly on the surface.

Key Words: **zirconia phases; alkali metal nitrate; nanosize crystals; zirconium chloride; molten salts.**

I. INTRODUCTION

Below 1170°C, the monoclinic polymorph of zirconia is the thermodynamically stable phase. Above, it turns into the tetragonal polymorph via a reversible martensitic transformation. The tetragonal structure is stabilized by doping agents, namely the alkali metal ions (1), or by different kinds of impurities, including the chloride ions (2). Moreover, for nanosized solids, the thermodynamic stability of the phases is affected. According to Garvie (3), as the ratio surface/volume increases, the tetragonal structure becomes the thermodynamically stable one for crystallite sizes lower than 30 nm. This critical value is determined considering the competition between bulk and superficial energies.

Molten alkali metal nitrates provide reacting liquid media in which numerous metal oxides (simples oxides as well as bi- or triconstituted ones) (4–7) can be prepared. Formally, the formation of the oxide occurs between the nitrate ions and the metal ions, but actually the other chemical species present in the system can take part in the reaction. Chemical reactions take place between a transition metal salt (precursor) and an excess of an alkali metal nitrate ANO_3 (molten salt). The nature of the alkali metal determines the physico-chemical properties of the ion (e.g., radius and ionic potential) and of the salt (e.g., acido-basic properties and melting points: $LiNO_3$, 255°C; $NaNO_3$, 307°C; and KNO_3, 334°C). The molten salt behaves as a Lux-Flood base (8) and dissociates via Eq. [1]. The alkali metal ions influence the basicity of the salt according to their ionic potential, the smallest, Li^+, leading to the highest basicity.

$$2ANO_3 \leftrightarrows 2A^+ + 2NO_2 + 1/2O_2 + O^{2-}. \qquad [1]$$

The influence of the precursor is studied by chosing $ZrCl_4$ and $ZrOCl_2.8H_2O$ as zirconium sources. According to Kerridge and Cancela-Rey (9), both react with nitrate ions, via respectively reactions [2] and [3], without involving the counteranions Cl^- nor the alkali metal cations. The zirconium cations behave as a Lux-Flood acid, the species exchanged in the acido-basic reaction being the oxide ion O^{2-}.

$$Zr^{4+} + 4NO_3^- \rightarrow ZrO_2 + 4NO_2 + O_2 \qquad [2]$$

$$ZrO^{2+} + 2NO_3^- \rightarrow ZrO_2 + 2NO_2 + 1/2O_2. \qquad [3]$$

In the tetrachloride, the structure is built up with zigzag chains of $ZrCl_6$ octahedra sharing one edge (10). There are obviously no pre-existing Zr–O bonds. The octahydrated zirconium oxychloride is constituted of individualized tetrameric entities $[Zr_4(OH)_8(H_2O)_{16}]^{8+}$ ($8Cl^-$, $12H_2O$) inside which the zirconium atoms are bridged by the hydroxyl groups and their octacoordination is supplemented by H_2O molecules (11). In this precursor, Zr–O bonds pre-exist and the local structure is not so far from that of zirconia, neither

[1]To whom correspondence should be addressed. Fax: 33 4 72 44 81 14. E-mail: deloume@univ-lyon1.fr.

0022-4596/02 $35.00

tetragonal because the coordination cube of oxygen is twisted, nor monoclinic because Zr is not heptacoordinated but octacoordinated.

ZrO_2 has been chosen to investigate the reciprocal influences of metal precursors and molten media on the physicochemical properties of oxides prepared in these media. Because of the existence of the monoclinic and tetragonal polymorphs, zirconia can reveal phenomena related to the above influences, favoring the formation of one crystalline variety rather than the other one.

II. EXPERIMENTAL PROCEDURE

$ZrOCl_2{\cdot}8H_2O$ is an analytical grade reagent commercially available (Fluka). $ZrCl_4$ was kindly provided by Cezus Chimie. Both were used as obtained. It is not possible to completely dehydrate the oxychloride without modifying its structure (11). The alkali metal nitrates are commercial salts (Prolabo Normapur). They are dehydrated for 24 hours at 120°C, and then preserved in a drying oven at 100°C.

The zirconium precursor is mixed with an excess of the alkali metal nitrate which constitutes the molten medium and the mixture is poured into the Pyrex glass reaction vessel. The ratio is estimated considering the stoichiometry of reaction [3] and, in agreement with previous works (12), stated at 8 NO_3^- per Zr. The proportion is the same at the beginning of the reactions and after completion the excess is 1.5 times lower for reaction [2] than for reaction [3].

All the reactions are performed at 450°C for various times. This temperature is high enough above the melting point of KNO_3 that the possible differences in viscosity between the various liquids ANO_3 may be neglected. An air or nitrogen flow is created in order to sweep away the exhausted gases. The temperature is raised, as usual, at a rate of $150°C.h^{-1}$ in two stages with a first intermediate level at 120°C for 1 hour in order to partially dehydrate $ZrOCl_2.8H_2O$ and a second level at 450°C for the reaction time. To maintain similarity in the process, the same heating profile is used in all reactions with $ZrCl_4$. At the end of the second level, the reaction molten medium is slowly cooled or quenched in air by taking out the reactor of the furnace. The solidified block is treated with water which dissolves all the salts but ZrO_2; this latter is filtered off, washed with water until elimination of Cl^- ions ($AgNO_3$ test), and finally oven dried at 100°C.

Zirconia powders have been characterized by following techniques: chemical analysis performed by the CNRS Central Service of Analysis at Vernaison, scanning electron microscopy (Hitachi S800 microscope, CMEAB of Claude Bernard University), thermal analysis (Setaram B70 digitalized thermobalance with a Pyrex glass crucible, Setaram 92-10 TA-DTA apparatus with an alumina crucible), isothermal adsorption of nitrogen (Carlo Erba Sorptomatic 1900), and X-ray diffraction (Siemens D500 diffractometer for powders working with Cu$K\alpha$ radiation, $\lambda = 1.5418$ Å, at the Henri Longchambon Center of Claude Bernard University).

The specific surface areas are calculated according to the BET equation. The XRD patterns are recorded in the 2θ range 20–50°; the diffractometer software refines the position of peaks, their middle height width, and the background. The peak areas are calculated maintaining the ratio between Lorentzian and Gaussian representations constant. For samples constituted of a mixture of monoclinic and tetragonal ZrO_2, the proportion is established using the equation proposed by Toraya (13):

$$\text{percent monoclinic} = \frac{1.311\,\dfrac{(I_{m11\bar{1}} + I_{m111})}{(I_{m11\bar{1}} + I_{t111} + I_{m111})}}{1 + 0.311\,\dfrac{(I_{m11\bar{1}} + I_{m111})}{(I_{m11\bar{1}} + I_{t111} + I_{m111})}}.$$

III. RESULTS AND DISCUSSION

III.1. Preliminary Investigations

A few experiments have been performed in order to ensure that some experimental parameters exert no influence on the characteristics of the obtained zirconia powders.

By performing the same experiment in reaction vessels made of different materials (Pyrex glass tube, alumina and zirconia crucibles), it is shown that the material has no influence on the nature of the phases obtained.

Comparing the results of two syntheses carried out under similar conditions, one involving anhydrous $ZrCl_4$ and the other hydrated $ZrCl_4$ (obtained by addition of water to the reaction medium in the proportion 8 H_2O per Zr, the same as in zirconium oxychloride), it is concluded that water not bound to zirconium has no influence on the phase obtained.

In previous work concerning the preparation of ZrO_2 by reaction of $ZrOCl_2{\cdot}8H_2O$ with molten equimolar $NaNO_3$–KNO_3 (mp 225°C) (12), a two-step transformation was evidenced by a weak emission of NO_2 below the melting point the nitrates mixture and then a strong release above the melting point. An experiment performed under the same conditions, but introducing the reaction mixture directly in a furnace preheated at 450°C, so as to by-pass the first step, shows that this latter does not determine the structure of the ZrO_2 obtained.

Last, a significant difference in the behavior of $ZrCl_4$ and $ZrOCl_2{\cdot}8H_2O$ is noticed. In about 10 minutes, the reaction of the former gives a precipitate with a totally clear supernatant whereas the reaction of the latter produces a paste-like medium releasing nitrogen oxides for more than 20 minutes.

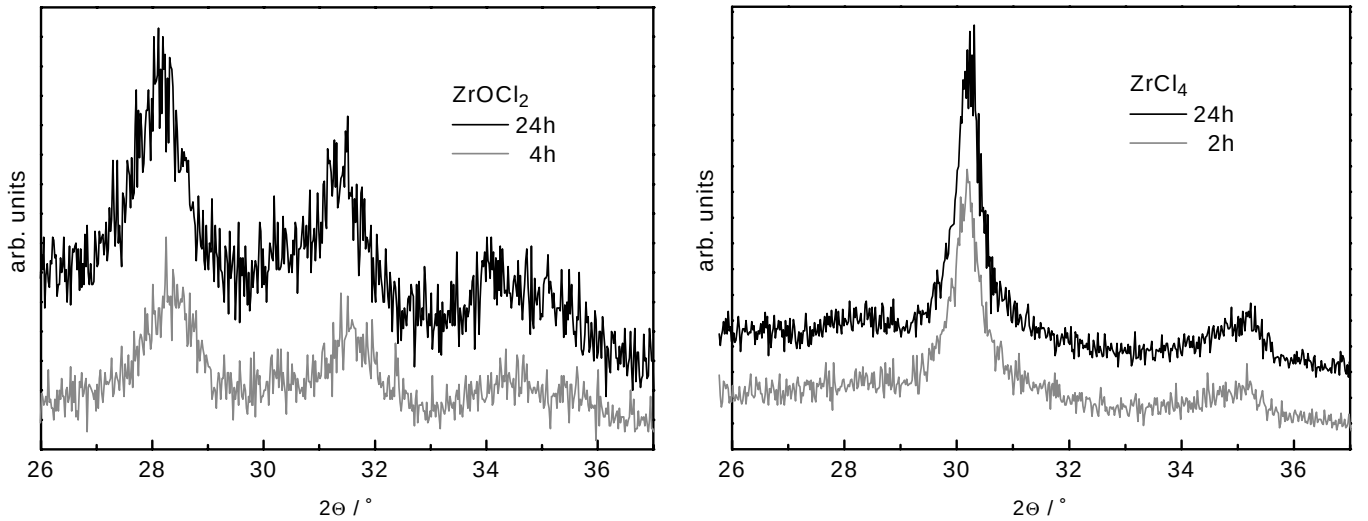

FIG. 1. Influence of the reaction time on the XRD patterns of zirconias prepared by reaction of $ZrOCl_2 \cdot 8H_2O$ or $ZrCl_4$ with respectively $LiNO_3$ and $NaNO_3$ at 450°C.

III.2. Obtained Phases and Size of Crystallites

The related results are mainly those obtained with two molten media, $LiNO_3$ and $NaNO_3$. In KNO_3 the results are indeed similar to those obtained in $NaNO_3$.

Whatever the zirconium precursor and the molten nitrate medium, the general trend is that the increase of the reaction time from 2 to 24 hours is not a prevailing factor in the balance between monoclinic and tetragonal zirconia (Fig. 1). Nevertheless, particularly for reactions carried out in $LiNO_3$ (Figs. 1 and 2), the use of $ZrOCl_2 \cdot 8H_2O$ promotes the formation of monoclinic ZrO_2 (% tetragonal < 10) whereas the use of $ZrCl_4$ favors the formation of tetragonal ZrO_2 (% tetragonal > 70). Coupled DTA–TG curves recorded for two zirconia samples prepared in $LiNO_3$, one from $ZrOCl_2 \cdot 8H_2O$ and the other one from $ZrCl_4$, do not show an exothermic peak about 400°C (12) corresponding to the crystallization of amorphous zirconia (Fig. 3).

For reactions performed in $NaNO_3$, the conclusion is the same, but the gap between the compositions of the powders according to the precursor is less.

The crystallite mean sizes determined from XRD peaks broadening using the Scherrer formula (Fig. 4) are always lower than 30 nm, e.g., the critical size proposed by Garvie for the thermodynamic stabilization of tetragonal ZrO_2 (3). Here also, the increase of the reaction time has no influence on the sizes. With the precursor $ZrOCl_2 \cdot 8H_2O$, relatively homogeneous sizes are obtained, the monoclinic crystallites (about 10 nm in $LiNO_3$, 8 nm in $NaNO_3$) exhibiting sizes

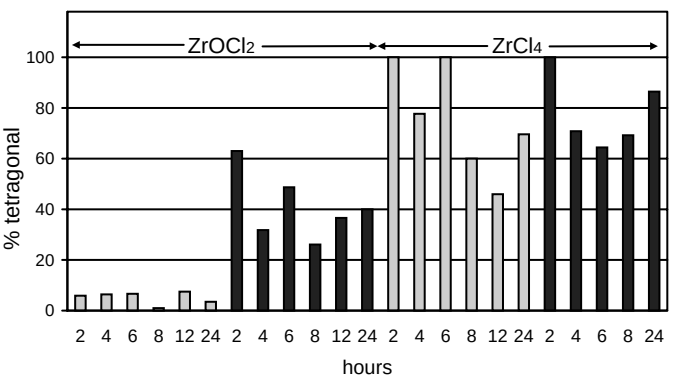

FIG. 2. Influence of the reaction time on the proportion between tetragonal and monoclinic phases in zirconias prepared by reaction of $ZrOCl_2 \cdot 8H_2O$ or $ZrCl_4$ with $LiNO_3$ (light gray) and $NaNO_3$ (black) at 450°C.

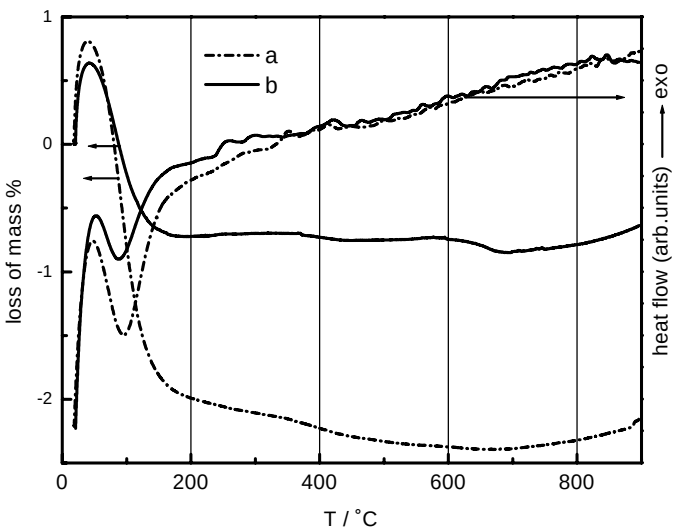

FIG. 3. Coupled DTA–TGA curves of zirconia powders prepared at 450°C in $LiNO_3$ for 2 hours from $ZrOCl_2 \cdot 8H_2O$ (a) or $ZrCl_4$ (b) (peak at 50°C corresponds to apparatus shift).

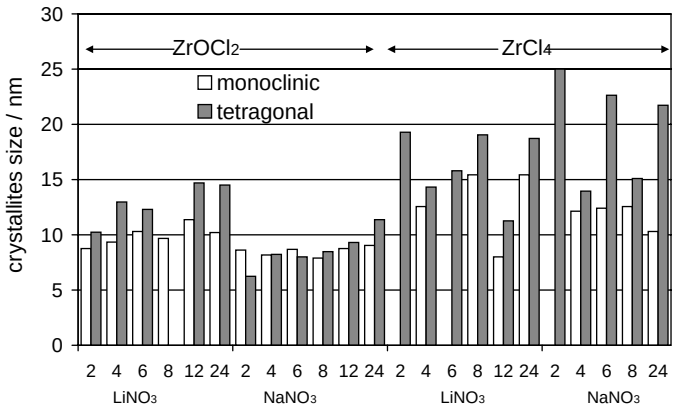

FIG. 4. Influence of the reaction time on the average sizes of tetragonal and monoclinic crystallites in zirconias powders prepared by reaction of $ZrOCl_2 \cdot 8H_2O$ or $ZrCl_4$ with $LiNO_3$ and $NaNO_3$ at 450°C.

comparable to those of the tetragonal ones (13 nm in $LiNO_3$, 8 nm in $NaNO_3$). With the precursor $ZrCl_4$, the crystallites are on average larger than the previous ones. However, the values are more dispersed. On the whole, the tetragonal crystallites (12–20 nm) are larger than monoclinic ones (8–16 nm).

III.3. Thermogravimetric Analysis of the Chemical Reactions

III.3.1. *Calcination of the precursors.* The calcination of the zirconium precursors in air at 500°C for 2 h (heating rate $150°C \cdot h^{-1}$) leads to tetragonal zirconia containing 2 at.% of chlorine. The average size of crystallites is 10 nm. For $ZrCl_4$ (Fig. 5), the experimental loss of mass, 115 $g \cdot mol^{-1}$ (51 mg from 103), is in satisfying agreement with that calculated from Eq. [4], 110 $g \cdot mol^{-1}$. It is the same for $ZrOCl_2 \cdot 8H_2O$ (Fig. 6), with an experimental value 195 $g \cdot mol^{-1}$ (41.9 mg from 69.7) very close to that calculated from Eqs [5] or [6], 193 $g \cdot mol^{-1}$. (The TGA experimental masses are corrected from the negative zero shift for the crucible by a factor 0.004 $mg \cdot {}^{\circ}C^{-1}$.)

$$ZrCl_4 + O_2 \rightarrow ZrO_2 + 2Cl_2 \qquad [4]$$

$$ZrOCl_2 \cdot 8H_2O \rightarrow ZrO_2 + 2HCl + 7H_2O \qquad [5]$$

$$ZrOCl_2 \cdot 8H_2O + 1/2O_2 \rightarrow ZrO_2 + Cl_2 + 8H_2O. \qquad [6]$$

3.2. Reactions with alkali metal nitrates. Whatever the Zr source is, its reactivity with the alkali metal nitrate is evidenced by a brown-red nitrogen dioxide emission which proves that nitrate ions are involved in the chemical reaction.

The thermogravimetric curves of the reaction mixtures $ZrOCl_2 \cdot 8H_2O$–alkali metal nitrate (40 mg of precursor), recorded from ambient to 500°C (Fig. 6), are in fair agreement with those previously published (12, 14) for the reaction of the oxychloride with equimolar $NaNO_3$–KNO_3 mixtures (mp 225°C). For the three alkali metal nitrates, the curves are similar to that of the decomposition of the precursor alone. A significant part of the loss (about three-fourths) is achieved below 200°C. The slope of curves then decreases and a quite linear evolution is observed up to 500°C which includes also the thermal decomposition of nitrates. At that temperature, the losses of mass are about 200 $g \cdot mol^{-1}$, but the reactions with the three nitrates are

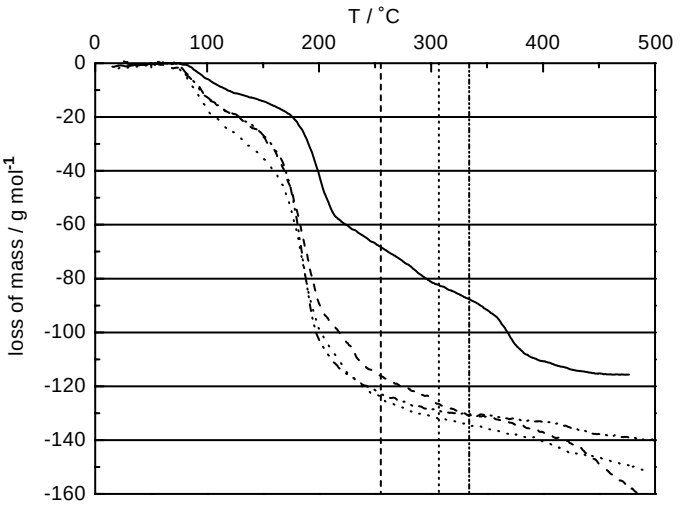

FIG. 5. TGA curves of the thermal decomposition of $ZrCl_4$ (solid line), the reaction of mixtures $ZrCl_4$–ANO_3 with A = Li (dashed line), A = Na (dotted line), and A = K (dash dot doted line). The vertical lines indicate the melting temperature of the corresponding nitrate.

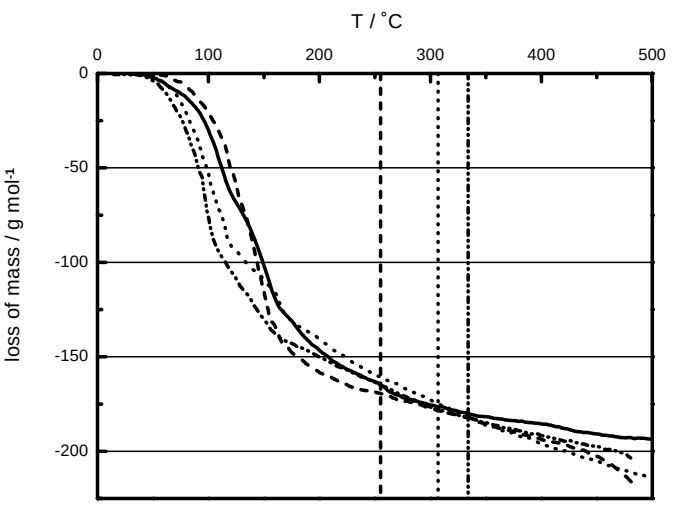

FIG. 6. TGA curves of the thermal decomposition of $ZrOCl_2 \cdot 8H_2O$ (solid line), the reaction of mixtures $ZrOCl_2 \cdot 8H_2O$–ANO_3 with A = Li (dashed line), A = Na (dotted line), and A = K (dash dot doted line). The vertical lines indicate the melting temperature of the corresponding nitrate.

TABLE 1
Experimental Loss of Mass (g) for Reactions of $ZrOCl_2 \cdot 8H_2O$ (2.6 g) with Alkali-Metal Nitrates, Performed at 450°C for 2 Hours under Different Conditions

	$LiNO_3$	$NaNO_3$	KNO_3
N_2 flow, level at 120°C for 1 h	1.828	1.834	1.797
Air flow, level at 120°C for 1 h	1.839	1.846	1.778
Air flow, without level at 120°C	1.839	1.806	1.776
Average value ($g.mol^{-1}$)	227	226	221

obviously not finished; the expected value 225 $g \cdot mol^{-1}$ is calculated from reaction [7].

To increase the accuracy of the loss of mass corresponding to complete reactions, experiments have been performed, at 450°C for 2 hours (general conditions) under different atmospheres, in test tubes with large amounts of reaction mixtures. The sets of results (Table 1) are homogenous. Neither the atmosphere nor the nature of the alkali metal ion has an influence on the loss of mass which closely agrees with the value of 225 $g \cdot mol^{-1}$. The atmospheric oxygen does not play any part in the reactions.

$$ZrOCl_2 \cdot 8H_2O + NO_3^- \rightarrow ZrO_2 + Cl^- + 1/2Cl_2 + NO_2 + 8H_2O. \quad [7]$$

The thermogravimetric curves of the reaction mixtures $ZrCl_4$–alkali metal nitrates (40 mg of precursor), recorded under the same conditions (Fig. 5), are similar for the three alkali metals but show losses of mass significantly higher than that obtained for the calcination of the zirconium salt alone. The main part of the loss occurs below the melting point of the nitrates and the reactions are not finished when the temperature reaches 500°C. As previously, experiments have been carried out at 450°C for 2 hours in test tubes. The reactions performed under a nitrogen flow give a loss of mass of about 171 $g \cdot mol^{-1}$. The reactions realized under an air flow produce a loss of mass close to 153 $g \cdot mol^{-1}$, significantly lower than that under nitrogen. Both results are a little higher than those calculated from reactions [8], 163 $g \cdot mol^{-1}$, and [9], 150 $g \cdot mol^{-1}$, respectively. In contrast to $ZrOCl_2 \cdot 8H_2O$, for which the results are generally lower than the expected ones, the values obtained here are higher; water adsorbed on the very hygroscopic $ZrCl_4$ could be responsible for that.

The value obtained under an air flow involves the participation of atmospheric oxygen to the chemical reaction.

$$ZrCl_4 + 2NO_3^- \rightarrow ZrO_2 + 2Cl^- + Cl_2 + 2NO_2 \quad [8]$$

$$2ZrCl_4 + 1/2O_2 + 3NO_3^- \rightarrow 2ZrO_2 + 3Cl^- + 5/2Cl_2 + 3NO_2. \quad [9]$$

III.4. Physico-chemical Characteristics of the Zirconias Obtained

Whatever the Zr source and the alkali metal are, the chemical analyses (Table 2) reveal zirconium amounts significantly lower than theoretical (74.0 wt.%). It is explained by the presence of water and small amounts of impurities. The determinations of hydrogen content lead to H/Zr atomic ratios in the range 0.5–0.8, proving that water is not completely eliminated by the oven-drying at 100°C or reabsorbed subsequently. Nitrogen and chlorine are present at about the same ratio in all the samples. Concerning the alkali metal, it is noticed first that their amount is about twice higher in the samples prepared from $ZrCl_4$ than in those prepared from $ZrOCl_2 \cdot 8H_2O$, second that Li atomic contents, probably because of its small size, are strongly higher than those of Na and K, and third that Na is present in samples obtained using $LiNO_3$ and KNO_3 reaction media. The presence of small amounts of Si (1 at.%) corroborates that in these latter samples Na results from the attack of the reaction vessel wall.

The precursor $ZrOCl_2 \cdot 8H_2O$ leads to ZrO_2 powders with much larger specific surface areas than $ZrCl_4$ (Table 3). These areas increase at the same time as the melting temperature of the nitrates.

The SEM micrographs reveal that $ZrOCl_2 \cdot 8H_2O$ is constituted of parallelepipedic crystals with a large distribution in size (Fig. 7a) and that the zirconias obtained from this precursor contain micronic agglomerates retaining the shape and the size of the smallest crystals of the oxychloride (Fig. 7c). Some of the biggest agglomerates (Fig. 7b) exhibit facets pearced by holes (arrows iii); they look like fragments of the largest oxychloride crystals (arrow i points at a cross section and arrow ii points at an edge of what could be the parent crystal). The formation of holes can be related to the gaseous release during the reaction. The larger the crystals,

TABLE 2
Chemical Analysis of Zirconia Powders Prepared from $ZrOCl_2 \cdot 8H_2O$ or $ZrCl_4$ by Reaction at 450°C for 2 Hours with $LiNO_3$, $NaNO_3$, or KNO_3[a]

	Zr	Li	Na	K	Cl	N
$ZrOCl_2 \cdot 8H_2O$						
$LiNO_3$	66.7	1.9	0.3		0.8	1.0
$NaNO_3$	61.5		0.7		1.6	1.1
KNO_3	64.5		0.7	0.5	0.8	2.4
$ZrCl_4$						
$LiNO_3$	69.4	3.4	0.6		1.3	0.9
$NaNO_3$	66.7		3.0		1.0	1.2
KNO_3	62.4		0.9	1.9	0.8	1.1

[a]Amounts are given in weight percent for Zr, atom percent for the other elements.

TABLE 3

Specific Surface Areas ($m^2 \cdot g^{-1}$) of Zirconia Powders Prepared by Reactions at 450°C for 2 Hours of $ZrOCl_2 \cdot 8H_2O$ or $ZrCl_4$ with $LiNO_3$, $NaNO_3$, or KNO_3

	$ZrOCl_2 \cdot 8H_2O$	$ZrCl_4$
$LiNO_3$	104	63
$NaNO_3$	140	61
KNO_3	204	91

the more significant the volume of gases released, so in small oxychloride crystals the gases diffuse whereas in the largest the pressure increases and the crystals explode.

The SEM micrographs of $ZrCl_4$ (Fig. 8a) show agglomerates with different shapes and sizes; the biggest ones exhibit spheroidal shapes and sizes in the range 10–20 μm. In the zirconia powders obtained by reaction with $ZrCl_4$ (Fig. 8b), the agglomerates are larger than those of the precursor and constituted of more angular particles.

III.5. Discussion

From a thermodynamic point of view, all the zirconia samples prepared by reaction with alkali metal nitrates exhibit crystallite sizes close to 10 nm, i.e., far below the critical size of 30 nm. Consequently, the powders should crystallize with only tetragonal symmetry.

Furthermore, it is well known that, whatever the size of crystallites is, tetragonal zirconia can also be stabilized by doping with elements of valency lower than four. Yttrium is the most frequently used for ceramic materials and oxygen sensors. In case of homogenous distribution, the formation of substitution solid solutions with anionic vacancies is commonly admitted (15). The stabilization by alkali metals has been less studied. Yet, it was observed that amorphous zirconia obtained by neutralizing zirconium oxychloride solutions by sodium hydroxide crystallizes in tetragonal or cubic zirconia according to their content in sodium when annealed (5, 16). Furthermore, cubic HfO_2 was obtained by reaction in solid state between $NaPO_3$ and Na_2HfO_3 (17) and by reaction of $HfCl_4$ with molten $NaNO_2$ (18). In the

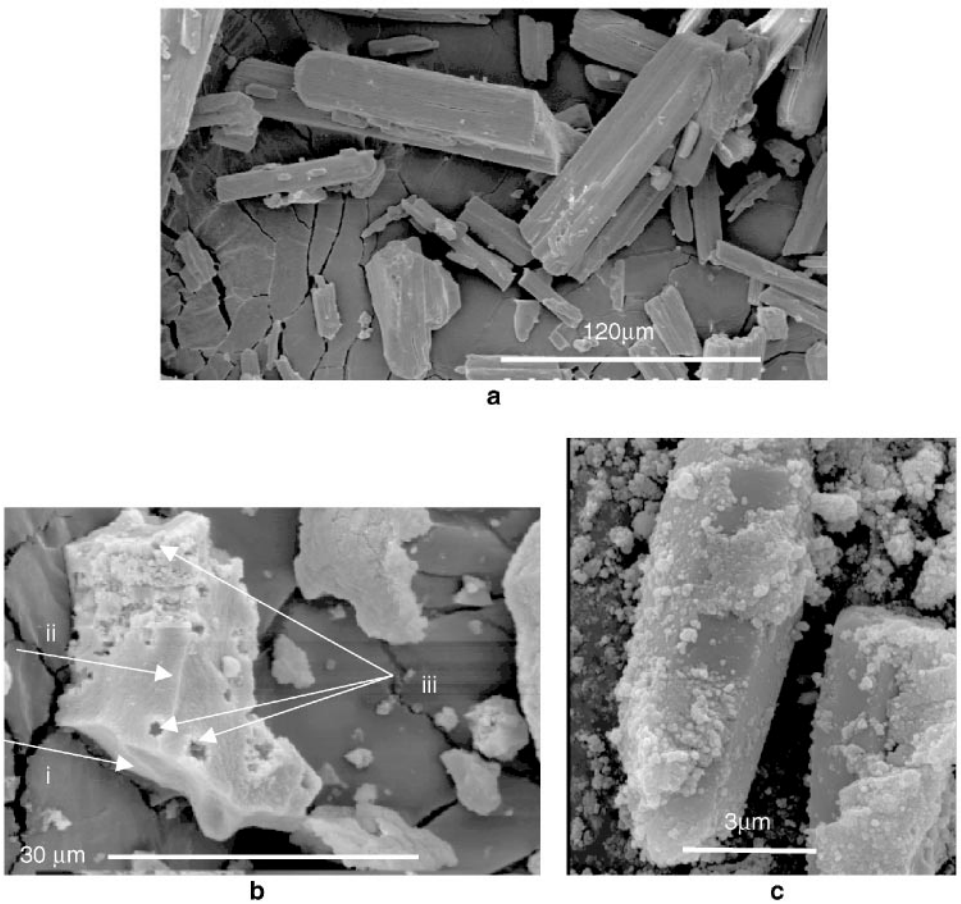

FIG. 7. Scanning electron micrographs of $ZrOCl_2 \cdot 8H_2O$ (a) and of the corresponding zirconia prepared by reaction at 450°C for 2 hours in $LiNO_3$ (b anc c). In (b) arrow i indicates a cross section, arrow ii indicates an edge of the parent crystal, and arrows iii point at the holes created by the evolution of the gases.

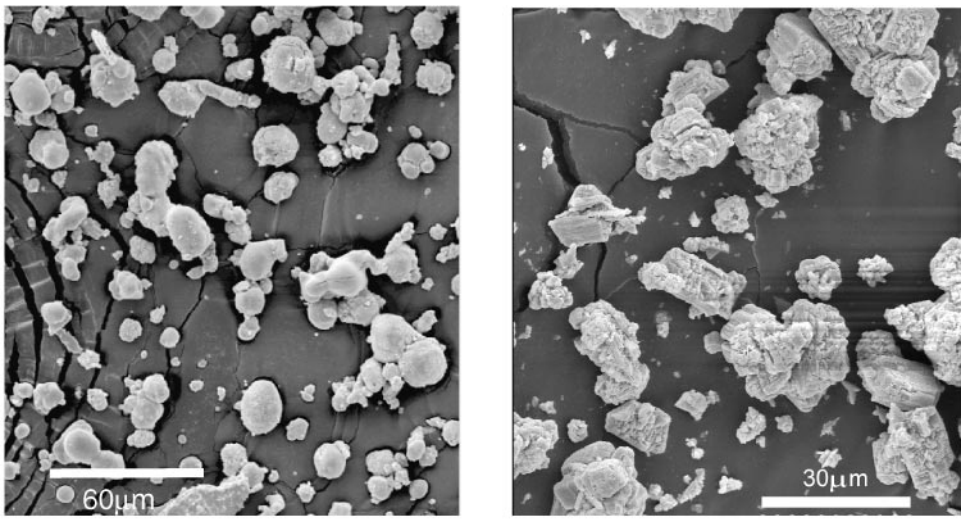

FIG. 8. Scanning electron micrographs of $ZrCl_4$ (a) and of the corresponding zirconia prepared by reaction at 450°C for 2 hours in $NaNO_3$ (b).

latter case, the stabilization is interpreted by the formation of a solid solution of Na_2O in HfO_2.

The differences in the structures of the two precursors or the presence of H_2O and OH^- in the oxychloride cannot be put forward. Indeed, for both precursors, the calcination in air leads only to tetragonal zirconia.

Above all, for the reactions involving the precursor $ZrCl_4$, the difference of basicity between the three alkali metal nitrates does not have a significant effect on the obtained polymorph, as shown in Fig. 2, for the reactions in $LiNO_3$ and $NaNO_3$.

The reasons for the formation of monoclinic zirconia, in more or less significant proportion beside the tetragonal polymorph, have to be searched for elsewhere.

Considering the reactions of the two studied precursors with the three alkali metal nitrates, the results presented above allow some assumptions to be made on the pathways to different zirconias. The presence of doping elements in the powders obtained is shown by chemical analysis and their distribution is a main factor. If they are homogeneously distributed inside the particles, the interactions created in the bulk prevail over the surface ones and the stabilization of tetragonal zirconia is favored. In contrast, if the doping element is predominantly localized close to the surface, only the superficial energy is modified. This can change the equilibrium between the bulk and surface to the benefit of the monoclinic phase.

When $ZrCl_4$ reacts, under inert atmosphere, with alkali metal nitrates above their melting temperature, no gas can escape spontaneously from its crystals. Nitrate ions then have to diffuse inside the crystals to form oxy compounds. The replacement of Cl^- by O^{2-} ions is a progressive reaction controlled by diffusion, with simultaneous elimination of the gas mixture $Cl_2 + NO_2$ via reaction [10]. If the pressure increases, the diffusion and consequently the reaction must slow down. The changes are drastic and the agglomerates are deeply modified. The alkali metal ions, which because electrostatic interactions accompany more or less the diffusion of nitrate ions, are trapped inside the structure. Their presence in the bulk stabilizes the tetragonal polymorph whatever the alkali metal is.

$$NO_3^- + Cl^- \rightarrow O^{2-} + 1/2Cl_2 + NO_2. \qquad [10]$$

When $ZrOCl_2 \cdot 8H_2O$ reacts under the same conditions, the increase of temperature brings about a significant release of H_2O and HCl vapors. The generated pressure, depending upon the size of the oxychloride crystals, leads to the explosion of the biggest ones. In every case, it causes a movement of matter, from the inside of the particles toward the outside, which goes against the diffusion of nitrate ions and alkali metal ions. The particles are surrounded by a gas shell in contact with the alkali metal nitrates in the solid or liquid state according to the temperature. According to Tosan's results (11) the loss of mass below 150°C corresponds to the evolution of five molecules of water; at this stage the global formula is $ZrOCl_2 \cdot 3H_2O$. Above, HCl begins to appear with the remaining quantity of water. Those simultaneous departures can create a pastelike phase between lithium nitrate crystals and the "precursor." In this phase gaseous HCl is likely to react with the alkali metal nitrate via Eq. [11]. The variation of standard free enthalpy, $\Delta rG^\circ \simeq -13 kJ \cdot mol^{-1}$ at 200°C (19), makes it possible to consider this redox reaction which agrees with the conclusions of TGA investigations. It would explain that the thermogravimetric curves of the reactions of the

oxychloride with the nitrates follow the decomposition of the precursor alone. The regular formation of a gas shell, all along the decomposition of the oxychloride, would also explain that the solid particles do not settle before complete transformation.

$$LiNO_3(s) + 2HCl(g) \rightarrow LiCl(s) + H_2O(g) + 1/2Cl_2(g) + NO_2(g) \quad [11]$$

As a confirmation of this pathway, the ZrO_2 powders are very porous and develop large specific surface areas.

According to this pathway, the alkali metal ions must be distributed mainly on the surface of crystallites of ca. 10 nm in size. As the TGA curves do not depend on the alkali metal nitrate, the difference of phase, according to the nature of the alkali metal, is interpreted by taking into account their ionic potential. The most polarizing one, the Li^+ ion, creates tensions on the surface of the particle which counteract the size effect. The equilibrium bulk/surface is then displaced toward the monoclinic phase. Powders containing less than 10% of the tetragonal phase are obtained. As the radius of the alkali metal increases, the polarizing power of the ion decreases, and the cation-induced superficial tensions are weakened. The powders obtained using $NaNO_3$ or KNO_3 contain about 40% of the tetragonal phase. An experiment carried out with caesium nitrate corroborates that, in the obtained zirconia, the tetragonal phase is largely predominant.

IV. CONCLUSION

The transformation of a zirconium salt in the corresponding oxide by reaction with an excess of an alkali metal nitrate involves a multistep reaction, the first one(s) occurring in the solid state, before the melting of the nitrates, and the last one(s) above the melting point. For the former(s) which represent(s) 80% of the reaction, the structure and the composition of the transition metal precursor are determining elements for the nature of the phase obtained and for some of its physico-chemical properties. For the latter(s) it might be the same, but, due to the presence of the liquid phase, the partial dissolution of the remaining zirconium precursor cannot be set aside.

REFERENCES

1. A. Benedetti, G. Fagherazzi, and F. Pinna, *J. Am. Chem. Soc.* **72**(3), 467–469 (1989).
2. R. Cypres, R. Wollast, and J. Rauq, *Ber. Bent. Keram.* **40**(9), 527–532 (1963).
3. R. C. Garvie, *J. Phys. Chem.* **82**(2), 218–224 (1978).
4. V. Harlé, J. P. Deloume, L. Mosoni, B. Durand, M. Vrinat, and M. Breysse, *Eur. J. Solid State Inorg. Chem.* **31,** 197–210 (1994).
5. P. Afanasiev, *Mater. Lett.* **34,** 253–256, (1998).
6. J. P. Deloume, J. P. Scharff, P. Marote, B. Durand, and A. Aboujalil, *J. Mater. Chem.* **9**(1), 107–110, (1999).
7. R. Lyonnet, C. Ciaravino, P. Marote, J. P. Scharff, B. Durand, and J. P. Deloume, *High Temp. Mater. Processes* **3**(2), 269–278 (1999).
8. D. H. Kerridge, *in* "The chemistry of nonaqueous solvents" (J. J. Lagowski, Ed.), Vol. VB, p. 269. Academic Press, New York, 1978.
9. D. H. Kerridge and J. Cancela-Rey, *J. Inorg. Nucl. Chem.* **37,** 405 (1977).
10. B. Krebs, *Z. Anorg. Allg. Chem.* **378,** 263–272 (1970).
11. J. L. Tosan, Ph.D. Thèse, Université Claude Bernard Lyon 1, no. 125, 1991.
12. M. Jebrouni, B. Durand, and M. Roubin, *Ann. Chim. Fr.* **16,** 569–579 (1991).
13. H. Toraya, M. Yoshimura, and S. Somiya, *J. Am. Ceram. Soc.* **67**(6), C119–121 (1984).
14. P. Afanasiev and C. Geantet, *Mater. Chem. Phys.* **41,** 18–27 (1995).
15. Th. Proffen, R.B. Neder, and F. Frey, *Acta Cryst. B* **52,** 59 (1996).
16. H. Nishizawa, N. Yamasaki, K. Matsuoka, and H. Mitsushio, *J. Am. Ceram. Soc.* **65,** 343 (1982).
17. G. Tilloca, *J. Mater. Sci.* **30,** 1884 (1995).
18. A. Benamira, Ph.D. Thesis no. 304, Université Claude Bernard Lyon 1, France, 1997.
19. "Handbook of Chemistry and Physics," 76th ed. (D. R. Lide, Ed.). CRC Press, Boca Raton, FL, 1995–1996.